

# Bandwidth equalization of purely phase-sampled fiber Bragg gratings for broadband dispersion and dispersion slope compensation

Hojoon Lee

*Department of Information and Communication Engineering, Hoseo University,  
Asan, 336-795, Republic of Korea.  
[hojoon@office.hoseo.ac.kr](mailto:hojoon@office.hoseo.ac.kr)*

Govind P. Agrawal

*The Institute of Optics, University of Rochester, Rochester, NY 14627, USA.  
[gpa@optics.rochester.edu](mailto:gpa@optics.rochester.edu)*

**Abstract:** We propose a purely phase-sampled Bragg grating for dispersion and dispersion slope compensation by introducing a chirp in the grating period and coupling coefficient. The bandwidth of all reflected channels can be equalized by chirping the sampling period at the same time. We show that a trade-off exists between the linearity of dispersion slope and the equalization of reflection channel bandwidths and discuss how the values of the coupling coefficients can be optimized in practice to improve the device performance.

©2004 Optical Society of America

**OCIS codes:** (050.2770) Gratings, (060.2330) Fiber optics communication, (060.2340) Fiber optic components, (260.2030) Dispersion.

---

## References and links

1. R. Kashyap, *Fiber Bragg Gratings* (Academic Press, San Diego, CA, 1999).
2. V. Jayaraman, Z. M. Chuang, and L. A. Coldereen, "Theory, design, and performance of extended tuning range semiconductor lasers with Sampled Gratings," *IEEE J. Quantum Electron.* **29**, 1824-1834 (1993).
3. B. J. Eggleton, P.A. Krug, L. Poladian and F. Ouellette, "Long superstructure Bragg gratings in optical fibres," *Electron. Lett.* **30**, 1621-1623 (1994).
4. F. Ouellette, P. A. Krug, T. Stephens, G. Dhosi and B. Eggleton, "Broadband and WDM dispersion compensation using chirped sampled fiber Bragg gratings," *Electron. Lett.* **31**, 899-901 (1995).
5. H. Ishii, Y. Tohmori, T. Tamamura, and Y. Yoshikuni, "Super-structure grating (SSG) for broadly tunable DBR lasers," *IEEE Photon. Technol. Lett.* **4**, 393-395 (1993).
6. H. Ishii, F. Kano, Y. Tohmori, Y. Kondo, T. Tamamura, and Y. Yoshikuni, "Narrow spectral linewidth under wavelength tuning in thermally tunable super-structure-grating (SSG) DBR lasers," *IEEE J. Sel. Top. in Quantum Electron.* **1**, 401-407 (1995).
7. Y. Painchaud, A. Mailloux, H. Chotard, E. Pelletier, and M. Guy, "Multi-channel fiber Bragg gratings for dispersion and slope compensation," in *Proc. Optical Fiber Communication Conference* (Optical Society of America, Washington, DC, 2002) paper ThAA5.
8. A.V. Buryak and D.Y. Stepanov, "Novel multi-channel grating devices," in *Proc. of Bragg Gratings Photosensitivity, and Polling in Glass waveguides vol. 60 of TOPS series* (Optical Society of America, Washington, DC, 2001), paper BThB3.
9. A. V. Buryak, K. Y. Kolossovski, and D. Y. Stepanov, "Optimization of refractive index sampling for multichannel fiber Bragg gratings," *IEEE Quantum Electron.* **39**, 91-98 (2003).
10. J. E. Rothenberg, H. Li, Y. Li, J. Popelek, Y. Sheng, Y. Wang, R. B. Wilcox, and J. Zweiback, "Dammann fiber Bragg gratings and phase-only sampling for high channel counts," *IEEE Photon. Technol. Lett.* **14**, 1309-1311 (2002).
11. H. Lee and G. P. Agrawal, "Purely phase-sampled fiber Bragg gratings for broad-band dispersion and dispersion slope dispersion," *IEEE Photon. Technol. Lett.* **15**, 1091-1093 (2003).
12. H. Lee and G. P. Agrawal, "Add-drop multiplexers and interleavers with broad-band chromatic dispersion compensation based on purely phase-sampled fiber gratings," *IEEE Photon. Technol. Lett.* **16**, 635-637 (2004).

## 1. Introduction

Fiber Bragg Gratings (FBGs) developed during the 1990s have found applications in the fields of both optical communication systems and optical fiber sensors [1]. A superstructure grating is useful for wavelength-division multiplexing (WDM) because it can provide multiple, equally spaced, reflective channels [2]. Several such gratings have been developed using an amplitude sampling approach [3], [4]. However, in the other class of superstructure FBGs, multiple reflective channels are created through phase sampling because the required index modulation then scales with the number  $N$  of channels as  $N^{1/2}$ , rather than  $N$  as found in the case of amplitude sampling. The phase-sampling technique has been used with success for making tunable semiconductor lasers, and it can produce a FBG whose reflectivity is uniform across many WDM channels [5], [6].

Use of FBGs for multichannel dispersion and dispersion-slope compensation has attracted considerable attention in recent years [7]-[13]. Superimposed [7] or superstructure gratings [8]-[13] are most suitable for high-capacity WDM systems. However, a superimposed grating requires multiple exposures during fabrication. Recently, purely phase-sampled FBGs have been proposed for compensating the dispersion and dispersion-slope simultaneously by chirping both the grating period and the sampling period [11]-[13]. However, the bandwidth of reflected channels was not uniform and it decreased with increasing channel wavelength, an undesirable property.

In this paper, we propose a solution to this problem based on purely phase-sampled Bragg gratings. Our main idea consists of introducing a chirp in the coupling coefficient together with the grating period. We show that the bandwidth of all reflected channels can be equalized by chirping simultaneously the grating period, the sampling period and the coupling coefficients. As an example, we design a 10-cm-long grating with almost the same bandwidth for all channels and show that it can compensate dispersion and dispersion slope for 16 WDM channels with 100-GHz spacing.

## 2. Purely phase-sampled gratings with chirp in the coupling coefficient

We first show that both the dispersion and the dispersion slope can be compensated by using a purely phase-sampled FBG designed with a chirp in its coupling coefficient and grating period. Using the Fourier analysis, the effective mode index within the fiber core can be written as

$$\begin{aligned} n(z) &= n_0 + \Delta n_1 \operatorname{Re}\{\exp[i(2\beta_0 z + \phi(z))]\} \\ &= n_0 + \Delta n_1 \operatorname{Re}\left\{\sum_m F_m \exp[2i(\beta_0 + m\beta_s)z]\right\} \end{aligned} \quad (1)$$

where  $n_0$  is the average refractive index,  $\Delta n_1$  is the constant modulation amplitude,  $\beta_0 = \pi/A_0$ ,  $\beta_s = \pi/A_s$ ,  $A_0$  is the average grating period, and  $A_s$  is the period of the sampling function.

The phase-sampling function  $\phi(z)$  with period  $A_s$  determines the coupling coefficient  $\kappa_m$  that is periodic in frequency with the channel spacing  $\Delta\nu = c/(2n_0A_s)$ , where  $n_0$  is the average refractive index. To compensate dispersion, we design the phase profile such that  $|\kappa_m|^2$  changes linearly for all WDM channels. We refer to this linear change as a chirp in the coupling coefficient. The peak reflectivity can be calculated using the coupled-mode equations and is given by  $R_p = \sum \tanh^2(|\kappa_m|/L)$  where the coupling coefficient  $\kappa_m$  depends on the Fourier coefficient  $F_m$  as  $\kappa_m = \pi\Delta n_1 F_m/\lambda_B$ , where  $\lambda_B = 2n_0A_0$  is the Bragg wavelength.

To design a purely phase-sampled FBG such that  $|\kappa_m|^2$  varies linearly for all WDM channels, we use a multidimensional minimization algorithm [11]. We divide the sampling

period  $\Lambda_s$  into many small segments and choose a trial form of  $\phi(z)$ . We then calculate the partial coupling coefficient corresponding to each Fourier coefficient and compute the mean-square deviation from the ideal value. The algorithm changes  $\phi(z)$  iteratively to minimize the mean-square deviation. Figure 1 shows the optimized phase profile obtained using only 20 segments. As shown there, the coupling coefficients  $|\kappa_m|^2$  for this phase profile vary almost linearly for 8 WDM channels.

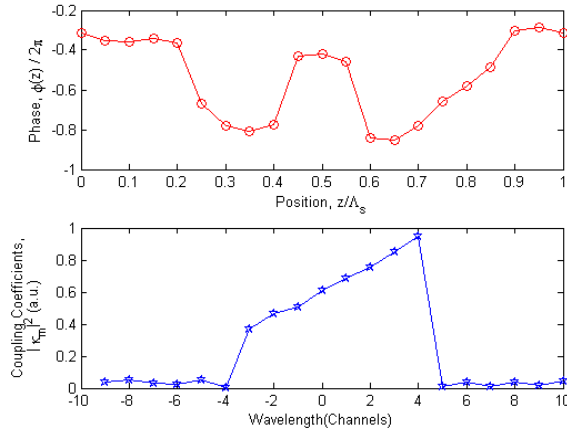


Fig. 1. Optimized phase profile (top) and the resulting of coupling coefficients (bottom) as a function of channel wavelengths for a 10-cm-long phase-sampled grating. Circles show the optimum phase values and stars denote the location of wavelength channels.

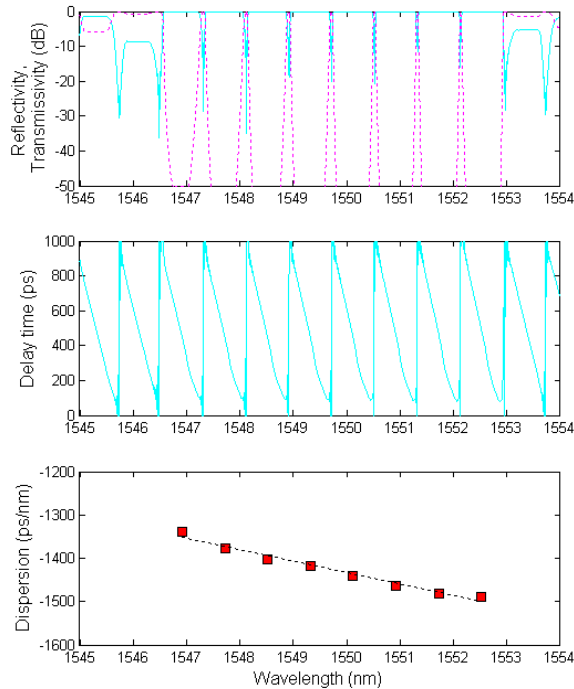


Fig. 2. Transmissivity (dotted line) and reflectivity (solid line) spectra (top) of the 10-cm-long grating. Delay time (middle) and dispersion values (bottom) obtained with the phase profile of Fig. 1 are also shown as a function of channel wavelength.

We show in Fig. 2 the transmissivity and reflectivity spectra, delay time  $\tau$ , and dispersion  $D = d\tau/d\lambda$  at the channel wavelengths, calculated numerically for the phase profile shown in Fig. 1 using a transfer-matrix approach. The grating parameters are chosen to be  $L = 10$  cm,  $\Delta n_1 = 7 \times 10^{-4}$  and  $\Lambda_s = 1$  mm. We also chirp the grating period at a rate  $\delta\Lambda_0 = 0.08$  nm/cm. To compensate for the dispersion slope, the phase profile shown in Fig. 1 (top) was used. We find that  $D$  changes linearly for all reflected channels and the slope of the dispersion is approximately  $26.8$  ps/nm<sup>2</sup>. Thus, such a grating with a chirp in the coupling coefficient can compensate for the dispersion slope. The reflectivity is almost 100% for all eight WDM channels. Indeed, the transmissivity of all reflected channels is below  $-50$  dB in Fig. 2. It is possible to increase the number of channels by changing the grating parameters.

Figures 3(a) and 3(b) show how the dispersion parameter  $D$  and the channel bandwidth vary with  $\Delta n_1$  while all other parameters are kept fixed and have the same values as in Fig. 2. It can be appreciated that, as  $\Delta n_1$  increases (that is, the magnitude of coupling coefficients increases),  $|D|$  as well as channel bandwidth increase for all WDM channels.

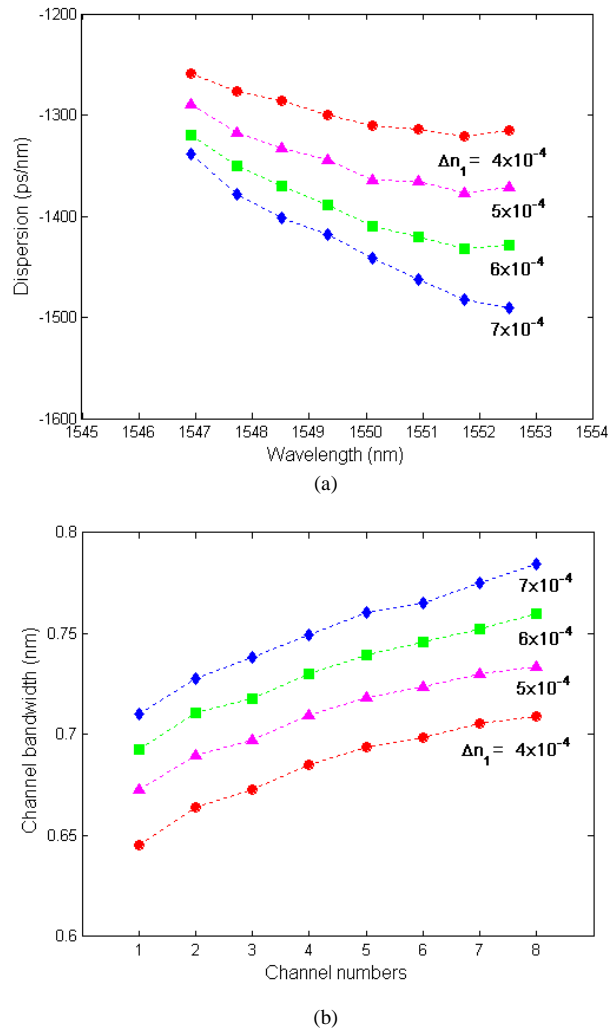


Fig. 3. (a) Dispersion parameter and (b) channel bandwidth as a function of channel wavelength for several values of modulation amplitude  $\Delta n_1$ . In all cases the coupling coefficients are chirped linearly.

### 3. Equalization of channel bandwidths

It is evident from Figs. 1-3 that both dispersion and dispersion slope can be compensated using a purely phase-sampled FBG when the coupling coefficient and the grating period are chirped as described above. However, the bandwidth is not uniform for all channels when this technique is used. For practical applications, the equalization of channel bandwidths is necessary. When dispersion slope is compensated by chirping the sampling period, the bandwidth decreases for longer wavelength channels [11]-[13]. On the other hand, when dispersion slope is compensated by chirping the coupling coefficients, the bandwidth of longer wavelength channel shows an increasing tendency. Therefore, we propose to equalize channel bandwidths by chirping the sampling period and the coupling coefficients simultaneously (in addition to the grating period).

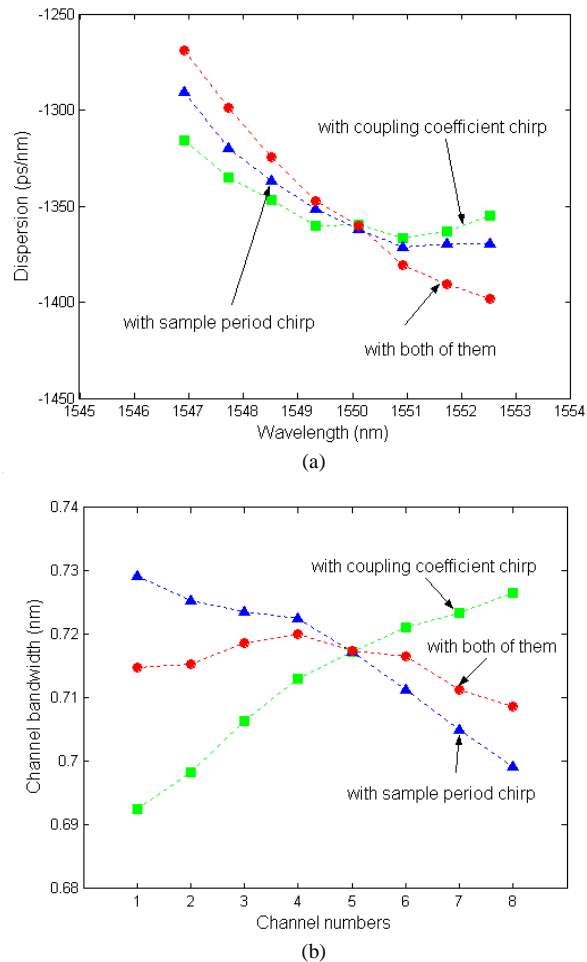


Fig. 4. (a) Dispersion parameter and (b) bandwidth of individual WDM channels when only the sampling period is chirped (blue triangles), only coupling coefficient is chirped (green squares), and both of them are chirped (red circles).

Figures 4(a) and 4(b) show the dispersion  $D$  and bandwidths as a function of channel wavelength, respectively, with  $\Delta n_1 = 5 \times 10^{-4}$  when (i) only sampling period is chirped, (ii) only coupling coefficient is chirped, and (iii) both are chirped. The magnitude of chirp in the sampling period was set at  $\delta\Lambda_s/\Lambda_s = 0.9\%$ . It can be seen from Fig. 4(a) that the case in

which both chirps exist simultaneously shows a sharper dispersion slope compared with the cases where a single chirp exists. Accordingly, when two chirps are used at the same time, the size of each chirp needs to be adjusted in conformity with the dispersion characteristics of the optical fiber. It can be seen from Fig. 4(b) that variations of the channel bandwidth show opposite behavior when either the sampling period or the coupling coefficient is chirped. However, channel bandwidth becomes nearly uniform when both quantities are chirped at the same time. Thus, such a scheme can compensate both the dispersion and dispersion slope, while maintaining a constant reflection bandwidth for all WDM channels.

Figures 5(a) and 5(b) show variations of  $D$  and channel bandwidth for four values of the modulation amplitude when both the coupling coefficient and the sampling period are chirped. As described above, as modulation amplitude increases, dispersion becomes more negative and bandwidth increases. However, for each value of modulation amplitude, the bandwidth of all channels remains nearly constant. Such a grating with  $\Delta n_1 = 5 \times 10^{-4}$  can compensate dispersion of 8 WDM channels with 100-GHz spacing over 350 km of Corning LEAF fiber, while providing almost the same reflection bandwidth for all channels.

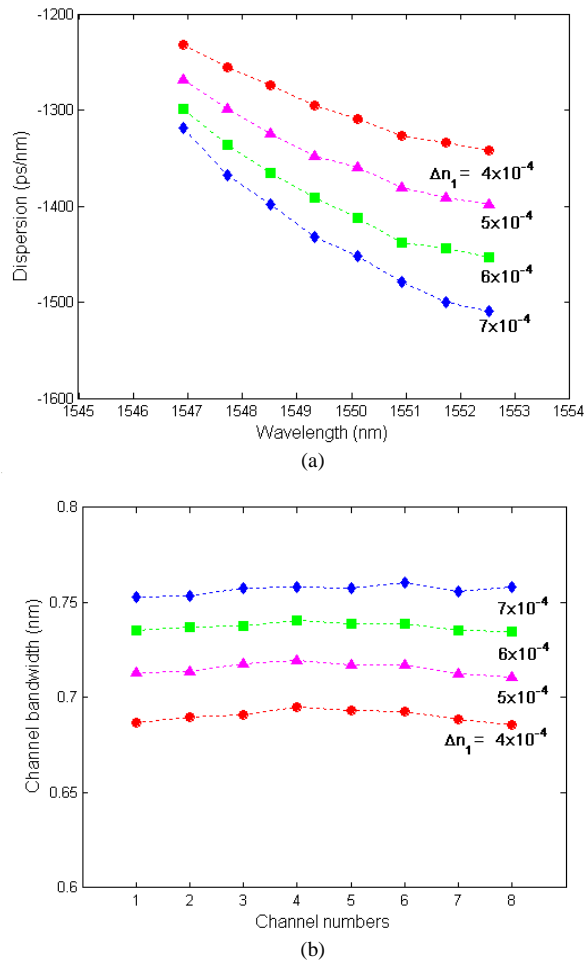


Fig. 5. (a) Dispersion  $D$  and (b) bandwidth of individual WDM channels for several modulation amplitudes when the coupling coefficient and the sampling period are chirped simultaneously.

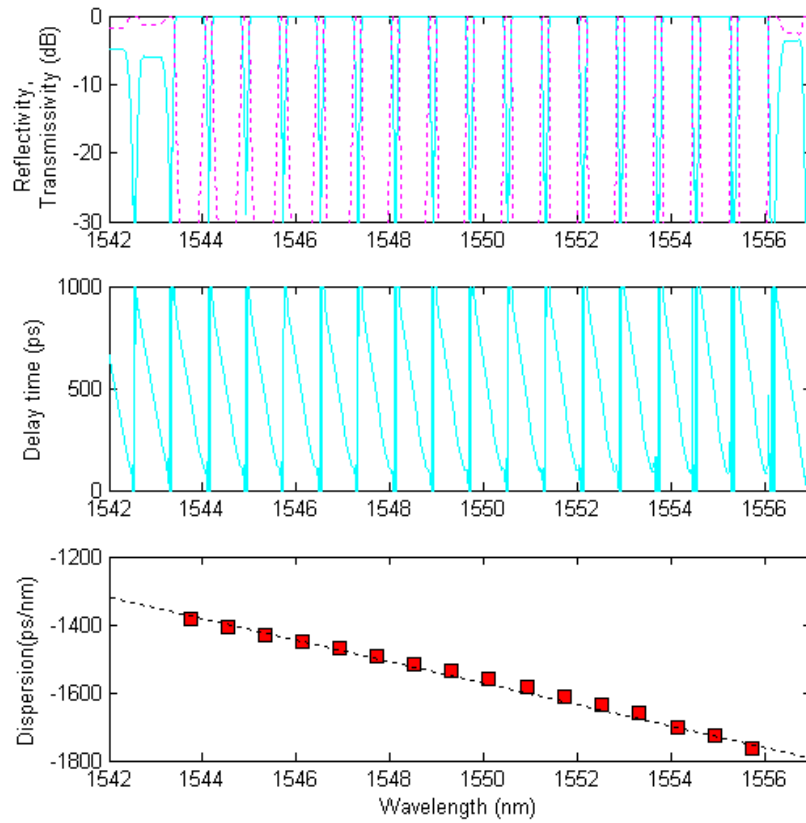


Fig. 6. Transmissivity (dotted line) and reflectivity (solid line) spectra (top) of a 10-cm-long grating designed for 16 WDM channels. Delay time (middle) and dispersion values (bottom) are also shown as a function of channel wavelength.

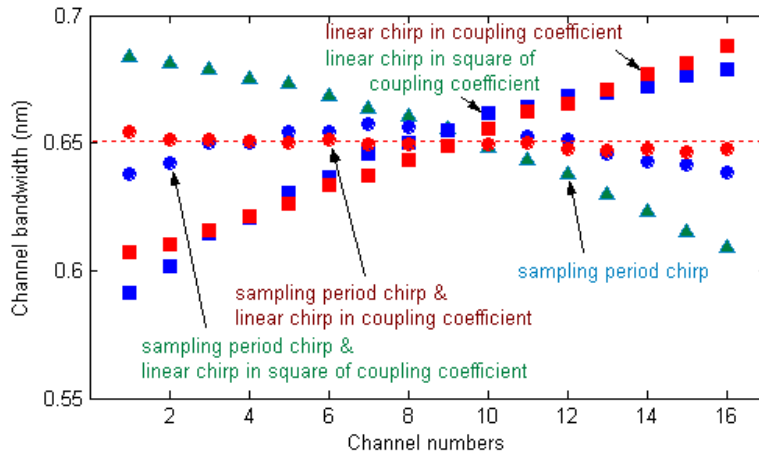


Fig. 7. Channel bandwidth for 16 WDM wavelengths when either the sampling period (triangles), or the coupling coefficient (squares), or both of them (circles) are chirped.

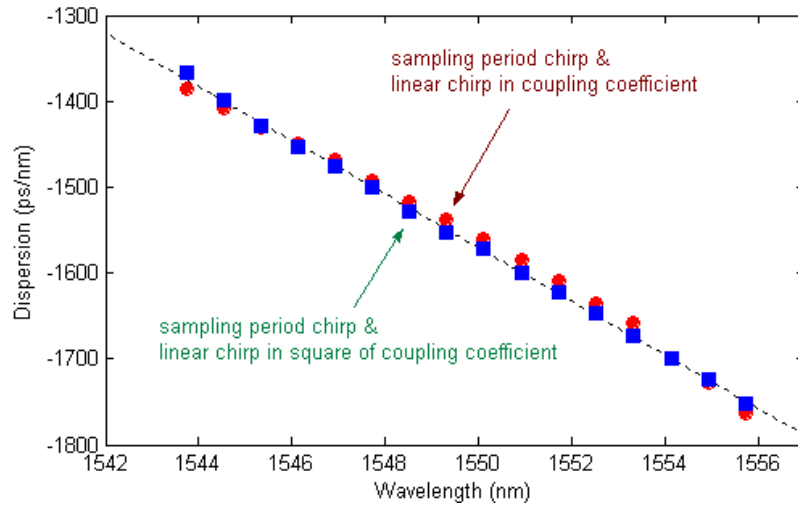


Fig. 8 The dispersion (a) and a channel bandwidth of individual WDM wavelength (b) at several modulation amplitude constants when the chirps in the coupling coefficient and the sampling period are generated at the same time, respectively.

Figure 6 shows our attempt to compensate the dispersion and dispersion slope of 16 channels simultaneously. A purely phase-sampled FBG is designed that  $|\kappa_m|$  (not  $|\kappa_m|^2$ ) changes linearly for WDM channels. The superstructure grating has the same parameters used for Fig. 5 except that  $\Delta n_1 = 8 \times 10^{-4}$ , and the chirps for the grating period and the sampling period were changed to  $\delta \Lambda_0 = 0.07$  nm/cm and  $\delta \Lambda_s / \Lambda_s = 1.0\%$ , respectively. Also, optimum phase profile was generated using 30 segments per sampling period. We find that  $D$  varies almost linearly for all reflected channels. Thus, such a grating with a linear chirp in the coupling coefficient can compensate for the dispersion slope.

To investigate the possibility of perfect bandwidth equalization, Figure 7 shows the channel bandwidths when (i) only sampling period is chirped, (ii) only coupling coefficient is chirped and (iii) both are chirped with. In this figure, we show two cases of the coupling coefficient chirp for which  $|\kappa_m|$  is either linearly chirped (red) or  $|\kappa_m|^2$  is linearly chirped (blue). We find that a constant reflection bandwidth for all WDM channels can be realized by introducing a linear chirp in  $|\kappa_m|$ . In contrast, a constant dispersion slope is obtained when  $|\kappa_m|^2$  is linearly chirped (see Fig. 8). Thus, a trade-off exists between the linearity of dispersion slope and the equalization of channel bandwidths. The maximum number of channels whose dispersion can be compensated simultaneously by using the proposed technique can be increased in practice by optimizing the chirp behavior of the coupling coefficients.

#### 4. Conclusions

In conclusion, we have demonstrated numerically that both the chromatic dispersion and the dispersion slope can be compensated by using purely phase-sampled superstructure FBGs, in which both the grating period and the coupling coefficient are chirped. We have also shown that channel bandwidths can be made uniform by chirping the sampling period appropriately. In general, a trade-off exists between the linearity of dispersion slope and the equalization of channel bandwidths.